

# Assessment of Tissue Iron Overload by Nuclear Magnetic Resonance Imaging

DONALD L. JOHNSTON, M.D., LAWRENCE RICE, M.D., G. WESLEY VICK, III, M.D., Ph.D., THOMAS D. HEDRICK, M.D., ROXANN ROKEY, M.D. *Houston, Texas*

**PURPOSE:** The ability of stored intracellular iron to enhance magnetic susceptibility forms the basis by which tissue iron can be detected by nuclear magnetic resonance (NMR) imaging. We used this technique to assess myocardial, spleen, and liver iron content in patients with known or suspected iron overload disorders.

**PATIENTS AND METHODS:** Spin echo NMR images were obtained in 30 patients; 20 had chronic anemias treated by multiple blood transfusions, five had idiopathic hemochromatosis, and five had non-hemochromatotic liver disease with elevated serum ferritin levels and no stainable iron on liver biopsy. The acquisition of oblique images through the short axis of the left ventricle permitted assessment of left ventricular function, while demonstrating the liver and spleen on the same image. Iron content was assessed using a signal intensity ratio of organ (spleen, liver, or myocardium) to skeletal muscle.

**RESULTS:** In patients with multiple blood transfusions, iron content was highest in liver, followed by the spleen. Significant iron overload was detected in the myocardium of only one patient. Left ventricular systolic wall thickening was normal in patients receiving multiple blood transfusions. Two patients with treated idiopathic hemochromatosis had normal signal intensity ratios, and three untreated patients had evidence of significant deposits of iron in the liver and spleen as indicated by a reduction in signal intensity ratios ( $0.2 \pm 0.01$  and  $0.9 \pm 0.01$ , respectively). Five patients with non-hemochromatotic liver disease and high serum ferritin levels had normal signal intensity ratios by NMR imaging.

**CONCLUSION:** NMR imaging is a useful method of detecting tissue iron and distinguishing disease due to iron overload. Myocardial iron deposition is a late event, occurring after accumulation of iron in the spleen and liver.

Patients with iron overload syndromes often exhibit clinical evidence of myocardial and hepatic involvement that, if untreated, terminates in fulminant cardiac or hepatic failure [1]. To prevent the development of iron-induced organ failure, it is necessary to make an early diagnosis of tissue involvement. However, it is not currently practical to assess iron content noninvasively, and tissue biopsy is required.

Nuclear magnetic resonance (NMR) imaging is a totally noninvasive technique that has been previously used to detect iron in the liver and brain [2-7]. Iron-containing substances like ferritin and hemosiderin become strongly magnetized when placed in a magnetic field [8-10]. This magnetization is quantified by the magnetic susceptibility, the ratio of the induced over the applied magnetic field. Localized regions of increased magnetic susceptibility selectively shorten relaxation time  $T_2$  by creating regions of magnetic field non-uniformity. As water molecules diffuse through these regions, there is irreversible spin dephasing, and enhancement of the  $T_2$  relaxation rate. Thus, following a radiofrequency pulse, recovery of transverse magnetization results in decreased signal intensity on spin echo images.

The aim of this study was to assess iron content of myocardium, spleen, and liver in patients with known or suspected iron overload disorders. A ratio of organ-to-skeletal muscle signal intensity was derived from NMR images to assess tissue iron content. Since excessive myocardial iron has a detrimental effect on cardiac function, myocardial thickening fractions were also derived from the NMR images.

## PATIENTS AND METHODS

### Patient Population

We studied 20 patients (nine females, 11 males) undergoing long-term blood transfusions for a variety of hematologic diseases. These included: sickle cell anemia (seven patients), end-stage renal disease (seven patients), myeloproliferative disorders (four patients), aplastic anemia (one patient), and sideroblastic anemia (one patient); three patients had prior splenectomy. Patients had received  $82 \pm 58$  (mean  $\pm$  SD) units of blood (total iron burden approximately 20 g) over one to nine years. Seven patients received less than 50 units ( $33 \pm 12$ ; range, 17 to 49), and 13 received 50 or more units ( $118 \pm 55$ ; range, 50 to 220). The mean age was 46 years and 48 years for patients receiving less than 50 units and 50 or more units, respectively. Ten patients who did not receive transfusions were studied. Five had idiopathic hemochromatosis, two of whom recently completed a course of therapeutic phlebotomies. Five other patients had hepatic disease with an elevated serum ferritin level, but no increase in stainable iron on liver biopsy. Eighteen normal sub-

From the Sections of Cardiology and Hematology, Department of Medicine, and the Department of Radiology, Baylor College of Medicine and The Methodist Hospital, Houston, Texas. Requests for reprints should be addressed to Donald L. Johnston, M.D., Section of Cardiology, Baylor College of Medicine, The Methodist Hospital, 6565 Fannin, MS 041, Houston, Texas 77030. Manuscript submitted November 1, 1988, and accepted in revised

tained to determine normal signal intensity ratios for heart, liver, and spleen. Fourteen of these subjects had images of the heart obtained at end-systole and end-diastole to derive values for normal cardiac function.

One transfusion recipient died eight weeks following NMR imaging, and the heart, liver, spleen, and skeletal muscle were excised and imaged post-mortem. Tissue iron was measured in this patient quantitatively by flameless atomic absorption spectrometry. In all other patients undergoing tissue biopsy, the material was stained for iron and qualitatively assessed.

### NMR Imaging Technique

Gated, spin echo images were obtained using a Siemens magnet operating at 0.5 tesla. All data were acquired in a  $128 \times 128$  matrix using two signal acquisitions. Time to echo (TE) was 35 msec, and the pulse repetition time (TR) was equal to the heart rate (mean heart rate = 71 beats/minute). This echo time produced a reasonable signal-to-noise ratio, but reduced the amount of blood flow signal normally associated with shorter echo times. To obtain short-axis images, a line was placed along the longitudinal axis of the left ventricle passing from the apex to the aortic outflow tract, and an angle was measured relative to the horizontal plane [11]. Since the Siemens imaging system did not permit imaging of more than one angle, a second angle was chosen by placing the patient in a  $30^\circ$  right anterior oblique position. A distance was measured between the base of the left ventricle and the apex to determine the length of the ventricle. With knowledge of ventricular length, it was possible to distribute basilar, mid, and distal slices evenly over the left ventricle. Images were obtained at end-diastole and end-systole using the imaging protocol described in Figure 1.

### Signal Intensity Measurements

Signal intensity measurements were made from a single image using a region of interest placed over the heart, spleen, liver, and skeletal muscle (latissimus dorsi). The slice chosen for these measurements was the mid-ventricular, end-systolic, short-axis image. In two studies, the latissimus dorsi was not well visualized on this slice, and measurements of muscle signal intensity were made from the basilar image of the same acquisition. To measure myocardial signal intensity, a transparent plastic sheet with six segments (anterior, anterolateral, posterolateral, inferior, inferior septum, and anterior septum) equally separated by  $60^\circ$  was placed over a magnified image of the heart. The mid-septum was identified as falling equal distance between the insertion of the superior and inferior right ventricular walls and was considered  $0^\circ$ . A circular region of interest was chosen to measure signal intensity for each of the six segments, and a single signal intensity value was obtained by averaging the segment values. For liver and spleen, the circular region of interest covered the largest possible area lying within the imaged organ. For skeletal muscle, three circular regions encompassing as much of the tissue as possible were averaged. The skeletal muscle was used as an internal standard to form a ratio with myocardium (myocardium/skeletal muscle), liver (liver/skeletal muscle), and spleen (spleen/skeletal muscle). A typical image demonstrating the location of the organs in the oblique plane is shown in Figure 2.

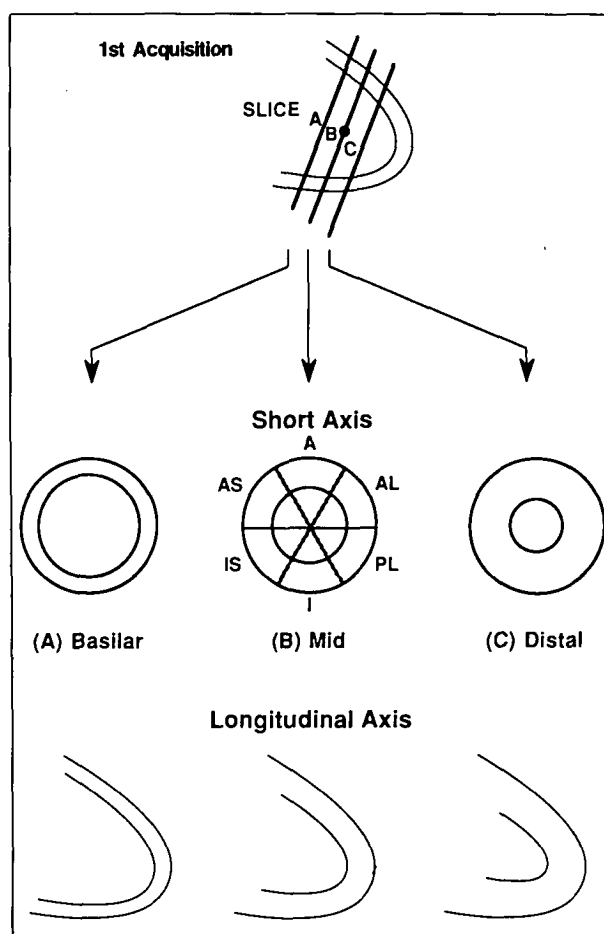


**Figure 1.** Position of the short-axis images was identified from the coronal image shown at the top of the figure. For the acquisition shown here, the basilar slice was obtained on the R wave of the electrocardiogram (end-diastole), and the distal slice was obtained on the downslope of the T wave (end-systole). The mid-ventricular slice was obtained midway between diastole and systole. The order of the second and third acquisitions was then rotated (2, 3, 1; 3, 1, 2). The mid, end-systole slice was subdivided into six segments for the purpose of assessing myocardial signal intensity. The basilar, mid, and distal slices were similarly subdivided to measure wall thickening. When time permitted, images were obtained at end-systole and end-diastole at three levels in the longitudinal axis of the left ventricle (bottom). A = anterior; AL = anterolateral; PL = posterolateral; I = inferior; IS = inferior septum; AS = anterior septum.

### Assessment of Cardiac Function

Left ventricular function was determined from the three NMR images passing through the basilar, mid, and distal portion of the left ventricle. The epicardial contour, including the right side of the interventricular septum and site of right ventricular insertions, and the endocardial contour, excluding the papillary muscles of the end-systolic and end-diastolic images, were traced onto a digitizing board. The center of geometry was a computer-derived, floating endocardial centroid from end-diastole to end-systole [12]. Each of the three slices was subdivided into six segments corresponding to the six segments used to derive the signal intensity measurements. The mid septum was labelled  $0^\circ$ , and for each segment, five radii were placed in systole and diastole for a total of 30 radii per slice. The percent myocardial thickening fraction was determined as change in wall thickness from end-diastole to

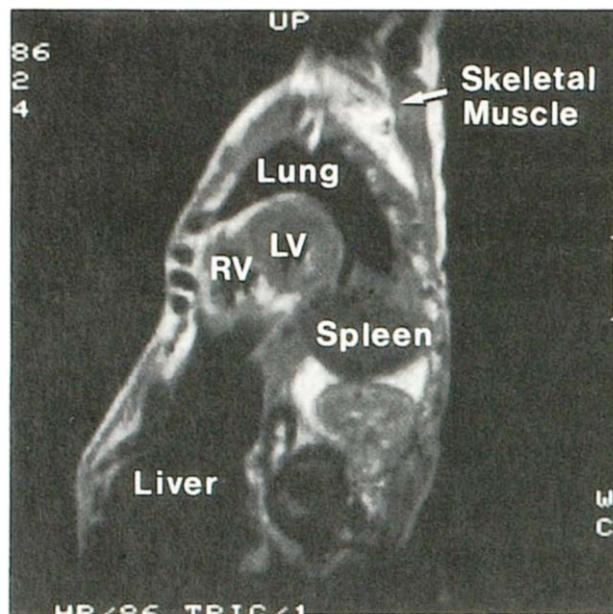


**Figure 2.** Short-axis image in a patient with iron overload showing the location of the liver, spleen, myocardium, and skeletal muscle in the oblique orientation. As demonstrated by this image, signal intensity of the liver was usually reduced more than that of the spleen or myocardium. This was observed in patients with both hemochromatosis and multiple blood transfusions. Since iron deposition is minimal in skeletal muscle in iron overload conditions, the latissimus dorsi was used as an internal standard for assessing organ signal intensity. RV = right ventricle; LV = left ventricle.

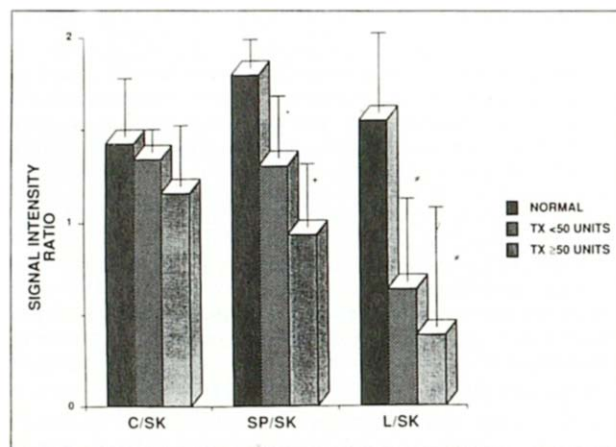


**Figure 3.** Relationship between signal intensity ratios for heart (C/SK), spleen (SP/SK), and liver (L/SK) and the number of blood transfusions received. Compared with ratios in normal subjects, a significant reduction in liver and spleen signal intensity ratios occurred for patients receiving multiple blood transfusions. Signal intensity ratios decreased as the number of transfusions increased (less than 50 units versus 50 units or more). C = cardiac; SK = skeletal muscle; SP = spleen; L = liver; TX = transfusions. \* =  $p < 0.05$ ; † =  $p < 0.01$ ; ‡ =  $p < 0.001$ , compared with normal values.

end-systole/end-diastolic wall thickness  $\times 100$ . Myocardial thickening fractions were summed for the 30 radii of each slice. The three slices were then summed (90 radii) to give a mean value for each patient. Left ventricular shortening fraction was determined as end-systolic chamber dimension/end-diastolic chamber dimension  $\times 100$ . Wall thickness was measured in

**TABLE I**

**Signal Intensity Ratios of Patients with Idiopathic Hemochromatosis or Liver Disease**

	Signal Intensity Ratios		
	Cardiac/Skeletal Muscle	Liver/Skeletal Muscle	Spleen/Skeletal Muscle
Normal subjects (n = 18)	1.40 $\pm$ 0.24	1.5 $\pm$ 0.14	1.9 $\pm$ 0.41
Hemochromatosis—untreated (n = 3)	1.3 $\pm$ 0.02	0.2 $\pm$ 0.01*	0.9 $\pm$ 0.01*
Hemochromatosis—treated (n = 2)	1.3 $\pm$ 0.7	1.0 $\pm$ 0.6	1.9 $\pm$ 0.1
Liver disease not due to iron overload (n = 5)	1.4 $\pm$ 0.2	1.4 $\pm$ 0.5	1.8 $\pm$ 0.7

\*  $p < 0.001$ , compared with normal subjects.

diastole and systole by making a single measurement from the anterior segment of the mid-left ventricular slice. Regional wall motion abnormalities were determined by visually assessing wall thickening at end-systole on the basilar, mid, and distal NMR images.

**Statistics**

Signal intensity ratios, left ventricular chamber dimensions, and wall thickening for normal subjects and patients with iron overload were compared using the unpaired Student's t-test. The level of significance was set at 5%. Intraobserver and interobserver variabilities for signal intensity ratio measurements were determined from images of 10 patients with iron overload. The intraobserver measurements were made one week apart. Variability was considered the mean difference and standard deviation of the differences between paired measurements of signal intensity ratios.

**RESULTS**

**Normal Signal Intensity Measurements**

Signal intensity ratios obtained for heart, spleen, and liver were 1.41  $\pm$  0.24, 1.92  $\pm$  0.41, and 1.54  $\pm$  0.14, respectively. Intraobserver variability for heart, spleen, and liver signal intensity ratios were 0.08  $\pm$  0.05, 0.07  $\pm$  0.08, and 0.08  $\pm$  0.06, respectively. Interobserver variability for heart, spleen, and liver signal intensity ratios were 0.14  $\pm$  0.12, 0.13  $\pm$  0.12, and 0.13  $\pm$  0.13, respectively.

**Patients Receiving Multiple Transfusions**

Signal intensity ratios obtained for heart, spleen, and liver were 1.23  $\pm$  0.22, 0.97  $\pm$  0.5, and 0.39  $\pm$  0.24, respectively ( $p = \text{NS}$ ,  $p < 0.001$ ;  $p < 0.001$ ; respectively, compared to normal values). These ratios indicated that the largest amount of iron was present in the liver. When the patients were divided into those who received less than 50 units of blood (n = 7) and those who received more than 50 units of blood (n = 13), myocardial, spleen, and liver signal intensity ratios were all lower for the latter group (Figure 3). Individual values lower than 2 SD below normal for heart, spleen, and liver (0.92, 1.08, and 1.22, respectively) were considered abnormal. For patients receiving less than 50 units of blood, myocardial, spleen, and liver signal intensity ratios were abnormal in zero, three, and seven

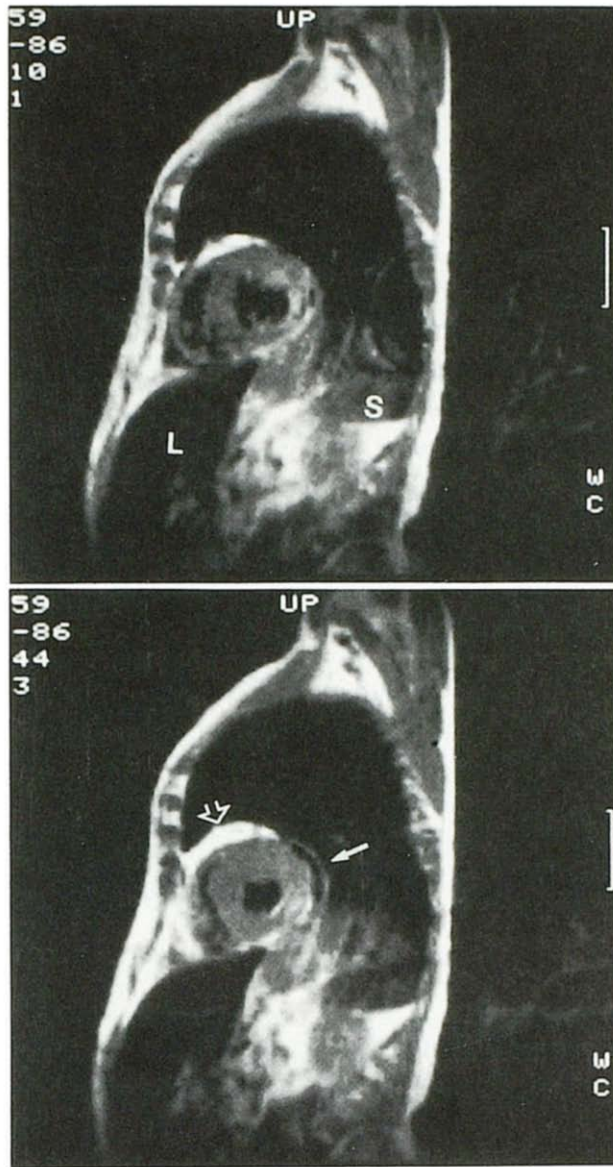


**Figure 4.** NMR images in a patient with untreated idiopathic hemochromatosis. **Top**, end-diastole; **bottom**, end-systole. The end-diastolic, anterior wall thickness measured 15 mm, indicating left ventricular hypertrophy. The inferoposterior wall was thinned in diastole and failed to thicken normally in systole, consistent with an old myocardial infarction. A small posterior pericardial effusion was present (**solid arrow**). The right ventricle was surrounded by fat (**open arrow**). Signal intensity values for myocardium, spleen (S), and liver (L) were 1.3, 0.94, and 0.25, respectively.

patients, respectively. For patients receiving 50 or more units, ratios were abnormal in one, 11, and 13 patients, respectively. Serum ferritin measurements for patients with multiple transfusions did not correlate significantly with liver signal intensity ratios.

#### Patients with Hemochromatosis or Other Liver Disease

The three patients with untreated idiopathic hemochromatosis had decreased spleen and liver, but normal myocardial signal intensity ratios (**Table I; Figure 4**). For the two patients who underwent therapeutic phlebotomies prior to imaging, signal intensity ratios were normal for all organs. Five patients



**Figure 5.** NMR images in a patient with liver disease and elevated serum ferritin level. All signal intensity ratios were within normal limits on the NMR scan, and no stainable iron was visualized on tissue obtained from liver biopsy. See Figure 4 for abbreviations.

had elevated serum ferritin levels (mean =  $1,348 \pm 743$  ng/mL) with evidence of liver disease biochemically as well as on liver biopsy. None of these patients had abnormal liver, spleen, or myocardial signal intensity ratios.

#### Patients Undergoing Tissue Biopsy

Five patients with multiple blood transfusions underwent liver biopsy and all had large amounts of stainable iron visualized. Consistent with the biopsy findings, mean liver signal intensity was markedly reduced ( $0.26 \pm 0.15$ ) for these five patients. All five patients with non-hemochromatotic liver disease and elevated serum ferritin levels underwent liver biopsy, and none had iron detected (**Figure 5**). One patient with decreased spleen and liver signal intensity ratios and a normal myocardial signal intensity ratio underwent right ventricular endocardial biopsy, and no stainable iron was present. *In vitro* signal intensity ratios obtained from the organs of the patient who died following NMR imaging correlated well with *in vivo* values (**Figure 6**).

#### Left Ventricular Function

To further document that the hearts of patients receiving multiple blood transfusions were not significantly involved by the process of iron loading, left ventricular function was examined using the NMR images obtained in the short axis (**Figure 7**). If measurement of signal intensity ratios underestimated the degree of iron loading, left ventricular function might be impaired and compensatory muscle hypertrophy might be expected [13]. There were no significant differences between patients with multiple transfusions and normal subjects in any functional parameters (**Table II**). When these parameters were compared in patients receiving a transfusion with either less than 50 units or 50 units or more, a trend emerged towards worsened function in the latter group; however, this

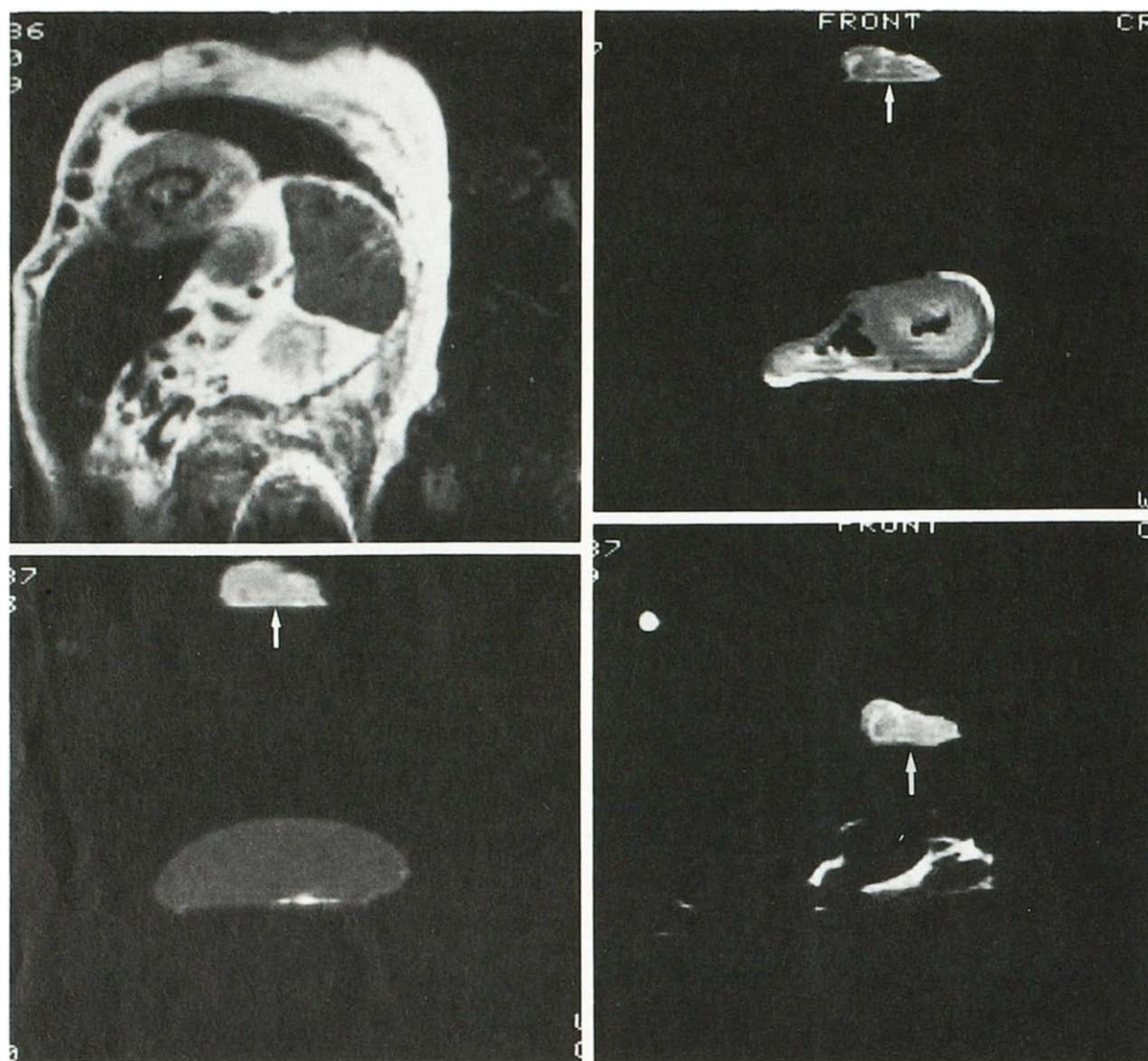


**Figure 6.** Correlation between the *in vivo* NMR image of iron overload in a patient who received multiple blood transfusions (top left) and *in vitro* NMR images at autopsy showing myocardium (top right), spleen (bottom left), and liver (bottom right). Skeletal muscle (arrow) was placed in the image plane and served as an internal reference. Signal intensity ratios obtained *in vivo* and *in vitro* (values in parentheses) were as follows: myocardium = 0.84 (0.81); spleen = 0.74 (0.89); liver = 0.16 (0.21). All values were 2 SDs below normal. Quantitative iron measurements were as follows (normal for liver = 530 to 900  $\mu\text{g/g}$  dry weight): myocardium = 2,272  $\mu\text{g/g}$  dry weight; spleen = 9,617  $\mu\text{g/g}$  dry weight; liver = 28,541  $\mu\text{g/g}$  dry weight. The smaller decrease in myocardial signal intensity corresponded to the smaller amount of iron measured quantitatively in the heart. In the excised heart image, endocardial signal intensity was greater than in the epicardium. This may have been due to the preferential iron deposition in the epicardium (decreased  $T_2$ ), or myocardial edema in the endocardium (increased  $T_2$ ) in association with the terminal illness, cardiogenic shock. Due to the effects of motion on image quality, it was not possible to clearly delineate differences in signal intensity between the epicardium and endocardium *in vivo*.

was not statistically significant (Table II). Two patients with multiple transfusions had regional wall motion abnormalities detected visually, one of whom had a previous history of myocardial infarction.

## COMMENTS

### Detection of Tissue Iron by NMR Imaging

The present study demonstrates the value of spin echo NMR imaging for assessing iron overload in the myocardium, liver, and spleen of humans. It also shows that an approximate estimate of iron stores can be made by comparing the signal intensity of the tissue with that of skeletal muscle, a structure that contains very little iron in iron overload states [13]. For patients

receiving multiple blood transfusions, the deposition of myocardial iron was insignificant compared with the amount of iron present in the liver and spleen. Myocardial iron deposition is most likely a late event in such patients. This was not unexpected since the reticuloendothelial system preferentially accumulates iron from breakdown of transfused red blood cells before deposition of iron occurs in the parenchymal cells of organs such as the heart. The results of another study examining hearts from autopsy subjects with iron overload of diverse origin were consistent with our findings [13]. These authors found that cardiac iron was always accompanied by heavy iron deposits in the liver and spleen, indicating that iron deposition in the

# Explore Litigation Insights

Docket Alarm provides insights to develop a more informed litigation strategy and the peace of mind of knowing you're on top of things.

## Real-Time Litigation Alerts



Keep your litigation team up-to-date with **real-time alerts** and advanced team management tools built for the enterprise, all while greatly reducing PACER spend.

Our comprehensive service means we can handle Federal, State, and Administrative courts across the country.

## Advanced Docket Research



With over 230 million records, Docket Alarm's cloud-native docket research platform finds what other services can't. Coverage includes Federal, State, plus PTAB, TTAB, ITC and NLRB decisions, all in one place.

Identify arguments that have been successful in the past with full text, pinpoint searching. Link to case law cited within any court document via Fastcase.

## Analytics At Your Fingertips



Learn what happened the last time a particular judge, opposing counsel or company faced cases similar to yours.

Advanced out-of-the-box PTAB and TTAB analytics are always at your fingertips.

## API

Docket Alarm offers a powerful API (application programming interface) to developers that want to integrate case filings into their apps.

## LAW FIRMS

Build custom dashboards for your attorneys and clients with live data direct from the court.

Automate many repetitive legal tasks like conflict checks, document management, and marketing.

## FINANCIAL INSTITUTIONS

Litigation and bankruptcy checks for companies and debtors.

## E-DISCOVERY AND LEGAL VENDORS

Sync your system to PACER to automate legal marketing.